for the first time to study the dynamics of annular prototropic tautomerism in a substituted pyrazole, namely crystalline 3,5-dimethylpyrazole, in which the most likely mechanism of proton transfer can be established. The compound forms trimers in the solid state held together by NH···N hydrogen bonding, and between 223 and 339 K the evidence is consistent with the tautomerism occurring by correlated triple proton jumps between the two equivalent or nearly equivalent forms of this structure; the rate constant follows the Arrhenius equation with an activation energy of 46 kJ mol^{-1} and a frequency factor of 10^{11} s^{-1}. There is a large kinetic hydrogen/deuterium isotope effect which is temperature dependent, $k_{12}^{HHH}/k_{12}^{DDD}$ being $\geq$20 at 299 K and equal to 8 at 347 K.

Other problems remain, such as the reason for the large isotope effect, and the question of whether or not other mechanisms such as tunneling or molecular librations occur at lower temperatures.[55] It would be important to have more information, both theoretical and experimental, on the shape of the potential energy surface and the effects of deuteration, as we have for the dimer of formic acid.[46] In future work, we hope to study these problems in more detail by means of ^{14}N, ^{15}N and ^{2}H spin-lattice relaxation and line shape measurements and fast field cycling ^{14}N studies at temperatures approaching the melting point.

Acknowledgment. We thank the European Community, the Deutsche Forschungsgemeinschaft, Bonn-Bad Godesberg, the Stiftung Volkswagenwerk, Hannover, and the Fonds der Chemischen Industrie, Frankfurt, the S.E.R.C. (U.K.), and the Pakistan Governments for financial support and research grants. We are also grateful to Dr. Paul Jonsen for a copy of his two-site exchange program, Dr. J. Shaw for performing the calculations, and T. J. Rayner for some of the ^{14}N spectra.

Supramolecular Structure and Microscopic Conformation of Cellulose Esters

Charles M. Buchanan,* John A. Hyatt, and Douglas W. Lowman

Contribution from the Research Laboratories, Eastman Chemicals Division, Eastman Kodak Company, P.O. Box 1972, Kingsport, Tennessee 37662. *Received December 12, 1988*

Abstract: Carbon-13 NMR relaxation studies and two-dimensional nuclear Overhauser exchange spectroscopy (NOESY) have been used to probe the effect of acyl group, temperature, and concentration on supramolecular structure and on the microscopic conformation of cellulose esters. Using these tools we show (i) the basic $^{4}C_{1}$ conformations of the anhydroglucose monomers are not affected by acyl type, temperature, or concentration, (ii) the virtual angle between H1 and H4′ of adjacent anhydroglucose units for cellulose esters is 30–34°, which suggests that these biopolymer derivatives exist as $^{5}/_{4}$ helices, (iii) cellulose triacetate undergoes a unique transition at 53 °C that is likely due to changes in supramolecular structure, and (iv) decreasing concentration induces a complex, interrelated change in both macromolecular order and microscopic conformation.

Cellulose esters have been known since 1869 and have been in commercial production since the first world war. Because of this long history, the art of synthesizing cellulose esters is well established. In contrast, due to the lack of suitable analytical techniques, our understanding of the basic relationships between macroscopic properties and the microstructure of these biopolymer derivatives is not nearly as developed, particularly in relationship to totally synthetic polymers and biopolymers such as proteins and nucleic acids. Application of suitable analytical techniques that would improve our understanding of microstructure of cellulose esters could very well lead to renewed growth in this extremely important class of materials.

Numerous studies have shown nuclear magnetic resonance spectroscopy (NMR) to be an indispensable tool for probing the microscopic behavior of a wide variety of synthetic polymers and biological macromolecules.[1] Recently, we provided NMR spectral assignments for cellulose triacetate (CTA, **1**), cellulose tri-

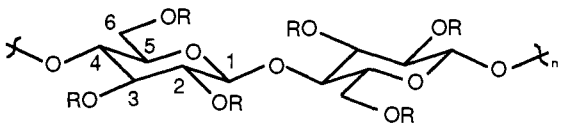

1 R = Ac
2 R = Pr
3 R = Bu

propionate (CTP, **2**), and cellulose tributyrate (CTB, **3**) and described methods by which detailed spectral information about these polymers could be obtained.[2] As a continuation of this work, we have searched for additional NMR techniques by which detailed information about the solution dynamics and conformations of these polymers could be obtained. In this regard, we have found carbon-13 (^{13}C) NMR relaxation time studies to be an excellent tool for probing the molecular dynamics of cellulose esters. In addition, we have coupled two-dimensional (2D) nuclear Overhauser exchange spectroscopy (NOESY) studies with the more established ^{13}C NMR relaxation time technique as a probe of the solution conformations of these macromolecules.

Our strategy in the first part of the work to be presented here was to examine the relaxation time behavior of CTA as a function of solvent, temperature, and concentration. We observed that CTA showed an unusual response to temperature and concentration, prompting comparison of the relaxation time behavior of CTP and CTB as a function of temperature to that of CTA. To determine if the observed changes in relaxation times were due to changes in microscopic conformation (in particular, changes in the virtual angle between adjacent anhydroglucose monomers) or changes in supramolecular structure, we measured the NOESY spectra of CTA, CTP, and CTB. Solution of the peak volume matrices gave the corresponding relaxation matrices at each mixing time for these polymers. The rate constants from these relaxation matrices were then used to calculate interproton distances.

Experimental Section

The preparation of the cellulose triesters and their NMR spectral assignments have been previously reported.[2] The samples were placed in either 5- or 10-mm NMR tubes and degassed by using the freeze-

(1) (a) Bovey, F. A. *High Resolution NMR of Macromolecules*; Academic Press: New York, 1972. (b) Wuthrich, K. *NMR in Biological Research: Peptides and Proteins*; American Elsevier Publishing: New York, 1976.

(2) (a) Buchanan, C. M.; Hyatt, J. A.; Lowman, D. W. *Macromolecules* **1987**, *20*, 2750–2754. (b) Buchanan, C. M.; Hyatt, J. A.; Lowman, D. W. *Carbohydr. Res.* **1988**, *177*, 228–234.

0002-7863/89/1511-7312$01.50/0

Table I. T_2 Values (seconds) for CTA at 100 MHz

			carbonyls			ring[a]					
concn, M	solvt	temp, °C	6	3	2	1	2	3	4	5	6
0.35	$CDCl_3$	25	0.24	0.29	0.18	0.03	0.03	0.03	0.03	0.03	0.05
0.35	DMSO-d_6	80	0.17	0.24	0.21	nm[b]	nm	nm	nm	nm	nm

[a] T_2 has been multiplied by the number of attached protons. [b] nm = not measured.

Table II. T_1 Values (seconds) for CTA at 100 MHz

			carbonyls			ring[a]					
concn, M	solvt	temp, °C	6	3	2	1	2	3	4	5	6
0.35	DMSO-d_6	80	2.87	1.95	2.84	0.25	0.27	0.23	0.22	0.19	0.22
0.35	DMSO-d_6	25	2.84	2.29	2.16	0.38	*b*	*b*	0.35	*b*	0.38
0.35	$CDCl_3$	25	2.16	1.62	1.93	0.31	0.28	0.29	0.30	0.30	0.32

[a] T_1 has been multiplied by the number of attached protons. [b] The resolution was insufficient for determination of T_1.

Table III. NOEF Values for CTA in $CDCl_3$ (25 °C)

			carbonyls			ring					
concn, M	solvt	freq, MHz	6	3	2	1	2	3	4	5	6
0.35	$CDCl_3$	67.9	0.0	0.11	0.32	0.68	1.09	0.53	0.42	0.92	0.57
0.35	$CDCl_3$	100	−0.12	−0.13	−0.10	0.46	0.55	0.56	0.54	0.56	0.25

Table IV. T_1 Values (seconds) for CTA at 67.9 MHz

			carbonyls			ring[a]					
concn, M	solvt	temp, °C	6	3	2	1	2	3	4	5	6
0.08	$CDCl_3$	33	2.19	1.53	1.96	0.22	0.19	0.21	0.18	0.18	0.21
0.17[b]	$CDCl_3$	33	2.54	1.91	2.13	0.20	0.20	0.19	0.20	0.19	0.20
0.35	$CDCl_3$	33	2.45	1.98	2.26	0.20	0.21	0.20	0.20	0.20	0.20
0.35	$CDCl_3$	45	2.71	1.95	2.39	0.21	0.21	0.20	0.20	0.20	0.22
0.35	$CDCl_3$	50	2.63	1.88	2.39	0.22	0.22	0.22	0.22	0.21	0.24
0.35	$CDCl_3$	53	3.00	2.44	2.70	0.13	0.13	0.13	0.13	0.13	0.13
0.35	$CDCl_3$	56	2.72	2.71	2.76	0.19	0.19	0.18	0.17	0.19	0.16
0.35	DMSO-d_6	35	2.59	2.36	2.21	nm	nm	nm	nm	nm	nm
0.35	DMSO-d_6	40	2.57	2.29	2.21	nm	nm	nm	nm	nm	nm
0.35	DMSO-d_6	45	2.56	2.27	2.22	nm	nm	nm	nm	nm	nm
0.35	DMSO-d_6	50	2.58	2.23	2.21	nm	nm	nm	nm	nm	nm
0.35	DMSO-d_6	53	2.56	2.23	2.23	nm	nm	nm	nm	nm	nm
0.35	DMSO-d_6	55	2.71	2.40	2.41	nm	nm	nm	nm	nm	nm
0.35	DMSO-d_6	60	2.71	2.40	2.50	nm	nm	nm	nm	nm	nm
0.35	DMSO-d_6	70	2.70	2.29	2.47	nm	nm	nm	nm	nm	nm

[a] T_1 has been multiplied by the number of attached protons. [b] Three experiments were done at this concentration and temperature. Percent deviation: carbonyls C6: 3.1, C3: 4.2, C2: 1.9; ring C1: 2.7, C2: 1.8, C3: 1.1, C4: 1.5, C5: 3.5, C6: 1.0. nm = not measured.

pump–thaw technique before sealing the tubes under an argon atmosphere. Molar concentrations are expressed in terms of moles of monomer.

Carbon-13 NMR data were obtained on either a JEOL Model GX-400 or GX-270 NMR spectrometer operating at 100 or 67.9 MHz, respectively. The inversion recovery method with complete decoupling of protons was used to collect spin–lattice relaxation times (T_1), and the Carr/Purcell/Meiboom/Gill sequence with complete decoupling of protons was used to collect spin–spin relaxation times (T_2). Carbonyl and ring carbon T_1 values were collected separately. CTA: For the ring carbons, the frequency window was 3538.6 Hz, the pulse delay was 4 s, and 512 scans were used to collect each spectrum. For the carbonyl carbons, the frequency window was 618.4 Hz, the pulse delay was 20 s, and 256 scans were used to collect each spectrum. CTP: The carbonyl spectral window was 326.1 Hz, the pulse delay was 16 s, and 224 scans were used to collect each spectrum. CTB: The carbonyl spectral window was 459.6 Hz, the pulse delay was 16 s, and 224 scans were used to collect each spectrum. For the variable-temperature T_1 experiments, the temperature variance was ±1 °C.

One-dimensional nuclear Overhauser enhancement factors (NOEF) were measured by using the gated decoupling technique. The experiments were conducted at ambient probe temperature using a pulse delay of 20 s.

A JEOL Model GX-400 NMR spectrometer operating at 400 MHz was used to collect NOESY spectra with the pulse sequence $(\pi/2)-t_1-(\pi/2)-\tau_m-(\pi/2)-t_2$. Absorption-mode phase-sensitive NOESY spectra were obtained by the method of States et al.[3] The NOESY spectra were collected by using a 1024 × 512 data matrix size, and 32 transients were acquired for each t_1 value. Spectral widths of 1812.9 (CTA), 1850.5 (CTP), and 2073.0 Hz (CTB) were used in both dimensions. The NOESY data were processed by using a Macintosh computer, with VersaTerm Pro (Version 2.0) as an emulation package, and Hare's FTNMR[4] software running on a VAX 8800 computer. Peak volumes were determined by using FTNMR software or by the method of Denk et al.[5]

Relaxation Studies

The basic theory of ^{13}C NMR relaxation times has been reviewed by a number of authors.[6] Although proton (^1H) NMR offers enhanced sensitivity relative to ^{13}C NMR, there are a number of reasons why ^{13}C NMR is the preferred technique for probing molecular dynamics of polymers in solution. One reason is the wider chemical shift range observed in ^{13}C NMR spectra (nearly 20 times that of ^1H NMR spectra), which leads to much better resolution of small structural details. The principal reason for choosing ^{13}C NMR is that relaxation is almost always dominated by dipolar interaction with attached protons and, with the exception of acetylenes, the C–H bond lengths are a constant value (1.09 Å). In contrast, ^1H NMR relaxation time values often

(3) (a) States, D. J.; Haberkorn, R. A.; Ruben, D. J. *J. Magn. Reson.* **1982**, *48*, 286–292. (b) Olejniczak, E. T.; Hoch, J. C.; Dobson, C. M.; Poulsen, F. M. *J. Magn. Reson.* **1985**, *64*, 199–206.

(4) Hare Research Inc., 14810 216th Av. N.E., Woodinville, WA 98072.

(5) Denk, W.; Baumann, R.; Wagner, G. *J. Magn. Reson.* **1986**, *67*, 386–390.

(6) (a) Breitmaier, E.; Spohn, K.-H.; Berger, S. *Angew. Chem., Int. Ed. Engl.* **1975**, *14*, 144–159. (b) Heatley, F. *Prog. NMR Spectrosc.* **1979**, *13*, 47–85. (c) Levy, G. C.; Lichter, R. L.; Nelson, G. L. *Carbon 13 Nuclear Magnetic Resonance Spectroscopy*; Wiley: New York, 1980.

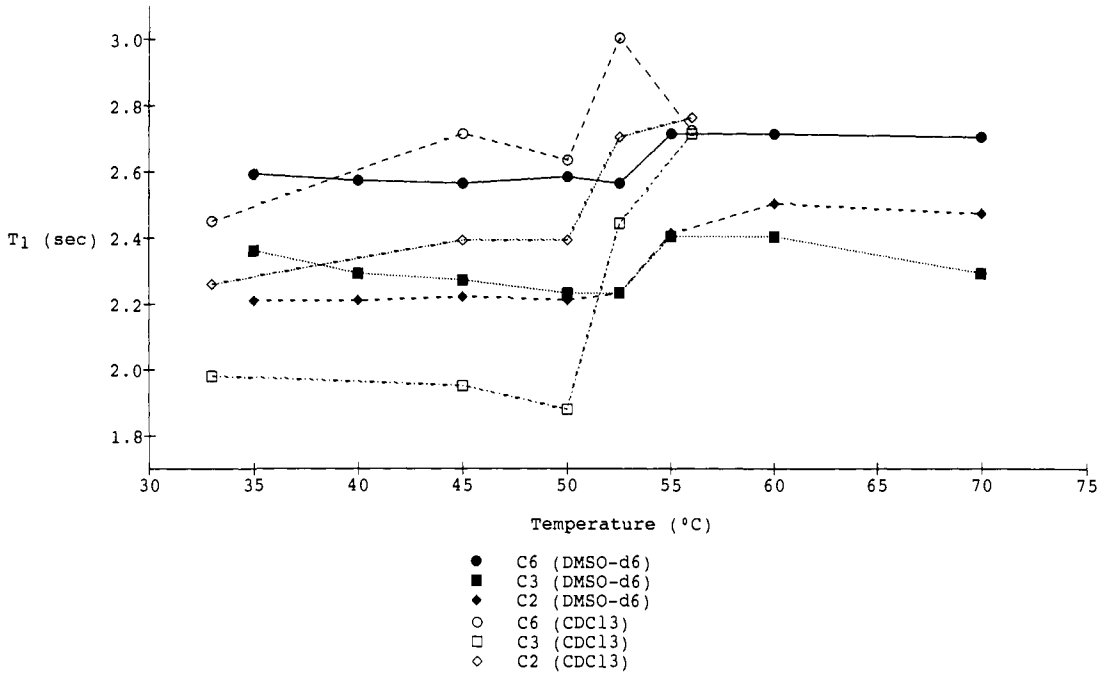

Figure 1. CTA carbonyl T_1 values (67.9 MHz).

Table V. T_1 Values (seconds) for CTP and CTB at 67.9 MHz in $CDCl_3$

ester	concn., M	temp, °C	carbonyls 6	3	2
CTP	0.30	40	3.28	2.66	2.33
CTP	0.30	45	4.10	3.23	2.77
CTP	0.30	50	4.06	2.76	2.49
CTP	0.30	55	3.45	2.42	2.42
CTP	0.30	60	2.94	2.04	2.27
CTB	0.27	40	2.45	1.94	1.97
CTB	0.27	45	2.81	2.16	2.28
CTB	0.27	50	2.52	1.83	2.33
CTB	0.27	55	2.70	1.93	2.22
CTB	0.27	60	2.51	1.76	1.94

contain contributions from nuclei varying distances away.

Tables I and II provide T_2 and T_1 values, respectively, at 100 MHz for CTA in $CDCl_3$ (25 °C) and DMSO-d_6 (25 and 80 °C). Table III lists NOEF values for CTA in $CDCl_3$ (25 °C) at 100 and 67.9 MHz. Table IV gives T_1 values for CTA in $CDCl_3$ at 67.9 MHz as a function of temperature and concentration and for CTA in DMSO-d_6 as a function of temperature. Table V gives T_1 values for the carbonyl carbons of CTP and CTB in $CDCl_3$ at 67.9 MHz as a function of temperature. Finally, entry 2 in Table IV provides a measure of the variance of the T_1 measurements.

Inspection of Tables I–IV provides a number of interesting insights into the molecular dynamics of CTA in solution. Comparison of T_2 and T_1 values (Tables I and II) for CTA at 100 MHz shows that the $T_{1,2}$ values differ in magnitude by a factor of ca. 10. The divergent nature of the T_1 and T_2 values indicates violation of the extreme narrowing limit, an observation borne out by the NOEF values in Table III. At 67.9 MHz the ring carbon NOEF values are reduced 45–80% from the maximum value of 1.98 and the carbonyl carbon NOEF values are vanishingly small. At 100 MHz, except for C3 and C4, the ring carbon NOEF values become even smaller while the carbonyl carbon NOEF values vanish. Moreover, the observation that the cross peaks are of the same phase as the diagonal peaks in the NOESY spectra of CTA also indicates slow overall reorientation of the polymer (vide infra). These observations suggest that the primary motion of the polymer in solution is anisotropic, which is consistent with cellulose esters existing in solution as extended rods.

One interesting observation we made with CTA in $CDCl_3$ (Table IV) was that in the temperature range 33–53 °C (vide infra) the carbonyl carbon T_1 values paralleled position reactivity reported for CTA in other solvent systems. (Studies[7] have shown that the reactivity of cellulose in acetylation and of CTA in hydrolysis follows the order, in decreasing order of reactivity, C6 > C2 > C3.) In DMSO-d_6, the parallel between carbonyl carbon T_1 values and position reactivity in other solvent systems is not nearly as clear cut. At all temperatures, the T_1 values of the C6 carbonyl carbon are larger than those for the C2 and C3 carbonyl carbons. Below 53 °C, the T_1 values for the C3 carbonyl carbon exceed those for the C2 carbonyl carbon. Above 53 °C, the situation is reversed; the C2 carbonyl carbon T_1 values exceed those of the C3 carbonyl carbon. In cellulose the observed reactivity has been attributed to primary hydroxyl versus secondary hydroxyl and to hydrogen bonding of the C3 hydroxyl to the ring oxygen of an adjacent anhydroglucose ring. However, hydrogen bonding is not possible for CTA. The higher reactivity of the C6 carbonyl relative to the C2 and C3 carbonyls can be attributed to a carbonyl attached to a primary hydroxyl versus carbonyls attached to secondary hydroxyls. However, there is no obvious reason for the difference between the reactivities of the C2 and C3 carbonyls in CTA hydrolysis.

Perhaps the most interesting observation was the significant effect of temperature and concentration on CTA T_1 values (Table IV). Decreasing the concentration or increasing the temperature effectively shortens correlation times and increases T_1 values.[6c] From Table IV we can see that for CTA in $CDCl_3$, decreasing the concentration while holding the temperature constant leads to a decrease in carbonyl carbon T_1 values while the ring carbon T_1 values remain constant. Conversely, increasing the temperature (Figure 1) at constant concentration ($CDCl_3$ or DMSO-d_6) has the opposing effect. In $CDCl_3$, there is a slight increase in T_1 values for the C6 and C2 carbonyl carbons and a slight decrease in the T_1 value for the C3 carbonyl carbon between 33 and 50 °C. Between 53 and 55 °C there is a large increase in T_1 values for all three carbonyl carbons until 56 °C, where all three carbonyl carbon T_1 values converge to the same point. The ring carbon T_1 values mimic the carbonyl carbons' T_1 temperature dependence. The ring carbon T_1 values remain constant until 53 °C, where they decrease nearly 50% in magnitude. At 56 °C, the ring carbon T_1 values return to near their former values. In DMSO-d_6, the carbonyl carbons exhibit the same pattern of behavior over this

(7) (a) Miyamoto, T.; Sato, Y.; Shibata, T.; Inagaki, H. *J. Polym. Sci., Polym. Chem. Ed.* **1984**, *22*, 2363–2370. (b) Wu, T. K. *Macromolecules* **1980**, *13*, 74–79.

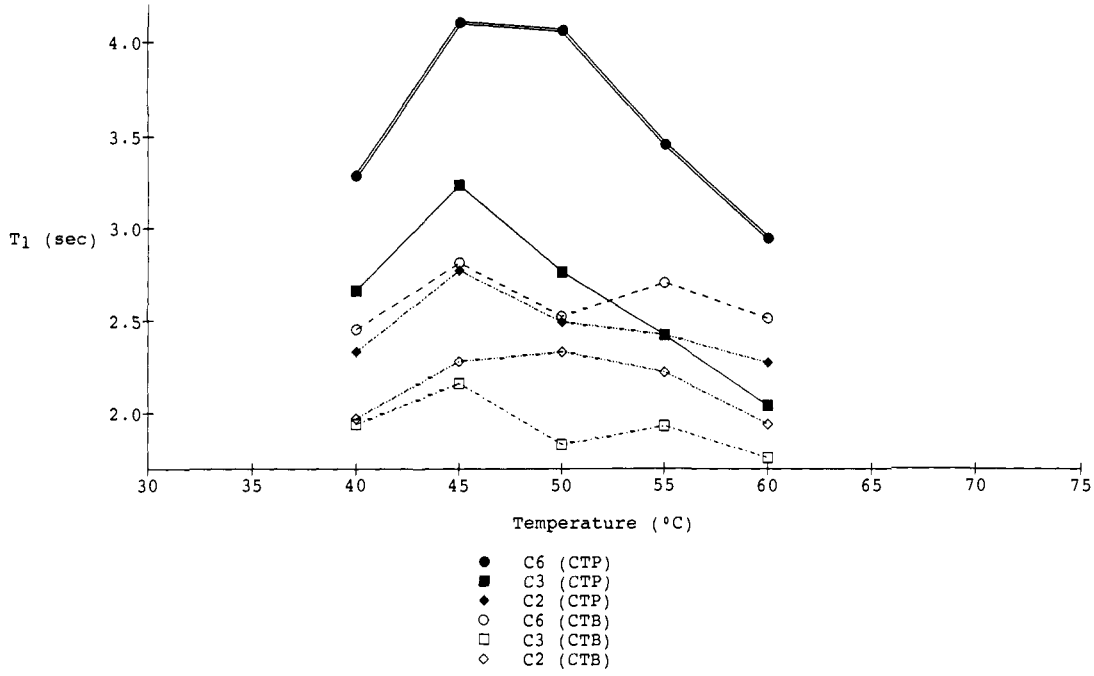

Figure 2. CTP and CTB carbonyl T_1 values ($CDCl_3$, 67.9 MHz).

Table VI. ^1H NMR Chemical Shifts and Coupling Constants for CTA, CTP, and CTB[a]

	CTA		CTP	CTB
	$CDCl_3$, 25 °C	$CDCl_3$, 60 °C	$CDCl_3$, 25 °C	$CDCl_3$, 25 °C
H1	4.42 (d, J = 7.9 Hz)	4.47 (d, J = 7.6 Hz)	4.35 (d, J = 7.9 Hz)	4.34 (d, J = 7.9 Hz)
H2	4.79 (t, J = 8.6 Hz)	4.78 (t, J = 8.2 Hz)	4.77 (t, J = 8.6 Hz)	4.76 (t, J = 8.6 Hz)
H3	5.07 (t, J = 9.0 Hz)	5.09 (t, J = 8.8 Hz)	5.07 (t, J = 9.1 Hz)	5.06 (t, J = 9.2 Hz)
H4	3.71 (t, J = 9.2 Hz)	3.72 (t, J = 9.2 Hz)	3.66 (t, J = 9.1 Hz)	3.61 (t, J = 9.2 Hz)
H5	3.53 (m)	3.57 (m)	3.47 (m)	3.48 (m)
$H6_S$	*b*	4.38 (d, J = 7.6 Hz)	*b*	*b*
$H6_R$	4.06 (m)	4.07 (m)	4.03 (m)	4.03 (m)

[a] All concentrations are 30 mg/mL. The data are taken in part from ref 2a. [b] $H6_S$ overlaps with H1.

temperature range except that the carbonyl carbon T_1 values do not converge to the same point above 55 °C.

We found the temperature dependence of the T_1 values for CTA to be quite intriguing, particularly the apparent transition at ca. 53 °C. This observation prompted us to examine the temperature dependence of the ^{13}C T_1 relaxation times of the carbonyl carbons of CTP and CTB. Figure 2 shows the T_1 values for CTP and CTB ($CDCl_3$) over the temperature range 40–60 °C. Apparently, these two closely related cellulose derivatives do not exhibit transitions between 53 and 55 °C. Finally, comparison of the carbonyl carbon T_1 values for each ester shows that the relative magnitudes of the T_1 values for CTA and CTB are similar whereas the values for CTP are considerably larger.

During the course of this work, Ryskina and Vakulenko[8] reported their studies on the solution conformation of CTA in acetic acid. On the basis of their studies using intrinsic viscosity, specific volume, optical rotation, absolute viscosity, and sorption of solvent measurements, they reported an abrupt change at 53 °C that they attributed to a change in conformation of CTA. Thus, by independent techniques from two different groups and in three different solvents, a transition is observed at ca. 53 °C that may possibly be related to the conformation of CTA. Moreover, the observed transition seems to be unique to CTA in that similar transitions are not observed with CTP or CTB in T_1 measurements. Certainly, one can relate the effect of temperature and concentration to polymer conformation. However, from the given data it is difficult to distinguish between changes in microscopic conformation (i.e., changes in monomer conformation or changes in the angle about the virtual bond connecting the monomers) and changes in supramolecular structure (i.e., changes in the interactions between polymer chains).

(8) Ryskina, I. I.; Vakulenko, N. A. *Polym. Sci. USSR* **1987**, *29*, 340–347.

NOESY Studies

The recent development of 2D NMR techniques has given the chemist a very powerful tool for the elucidation of the microstructure of biological macromolecules and synthetic polymers.[9] In this regard, one of the more promising techniques is NOESY spectroscopy, which measures the through-space interaction between spins.[10] For protons in macromolecular systems, the strength of through-space interactions depends upon the inverse sixth power of the distance between them. This allows the calculation of interproton distances, which can provide insight into the conformation of the polymer in solution at the microscopic level.

(9) (a) Bax, A. *Two-Dimensional Nuclear Magnetic Resonance in Liquids*; Delft University Press: Holland, 1984. (b) Morris, G. *Magn. Reson. Chem.* **1986**, *24*, 371–403. (c) Mirau, P. A.; Bovey, F. A. *Macromolecules* **1986**, *19*, 210–215. (d) Gippert, G. P.; Brown, L. R. *Polym. Bull.* **1984**, *11*, 585–592. (e) Scarsdale, J. N.; Prestegard, J. H.; Ando, S.; Hori, T.; Yu, R. K. *Carbohydr. Res.* **1986**, *155*, 45–56.

(10) (a) Mirau, P. A.; Bovey, F. A.; Tonelli, A. E.; Heffner, S. A. *Macromolecules* **1987**, *20*, 1701–1707. (b) Mirau, P. A.; Bovey, F. A. *J. Am. Chem. Soc.* **1986**, *108*, 5130–5134. (c) Kumar, A.; Wagner, G.; Ernst, R. R.; Wuthrich, K. *J. Am. Chem. Soc.* **1981**, *103*, 3654–3658. (d) Jansson, P.-E.; Kenne, L.; Wehler, T. *Carbohydr. Res.* **1987**, *166*, 271–282. (e) Bruch, M. D.; Bovey, F. A. *Macromolecules* **1984**, *17*, 978–981. (f) Dobson, C. M.; Olejniczak, E. T.; Poulsen, F. M.; Ratcliffe, R. G. *J. Magn. Reson.* **1982**, *48*, 97–110. (g) Macura, S.; Wuthrich, K.; Ernst, R. R. *J. Magn. Reson.* **1982**, *47*, 351–357. (h) Ellena, J. F.; Hutton, W. C.; Cafiso, D. S. *J. Am. Chem. Soc.* **1985**, *107*, 1530–1537. (i) Keepers, J. W.; James, T. L. *J. Magn. Reson.* **1984**, *57*, 404–426. (j) Johnston, E. R.; Dellwo, M. J.; Hendrix, J. *J. Magn. Reson.* **1986**, *66*, 399–409. (k) Perrin, C. L.; Gipe, R. K. *J. Am. Chem. Soc.* **1984**, *106*, 4036–4038. (l) Esposito, G.; Pastore, A. *J. Magn. Reson.* **1988**, *76*, 331–336.

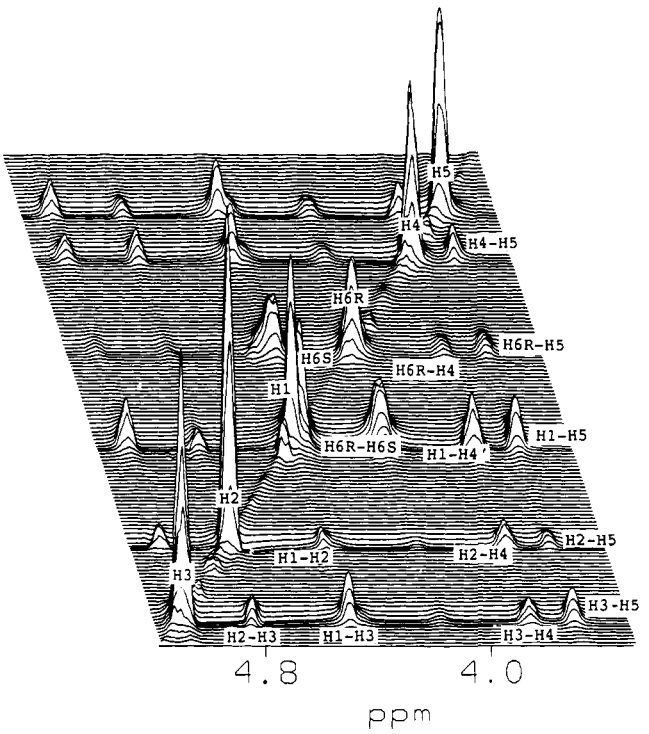

Figure 3. Stack plot of a NOESY spectrum for CTA (0.35 M, 25 °C) at a mixing time of 100 ms. The F_1 and F_2 axes are equal.

As with 1D NOE, NOESY has mainly been used as a qualitative tool. However, recent work has led to the development of methods that allow NOESY to be quantitatively utilized.[10a-c,f,l] The approach we have adopted is similar to that of Mirau et al.[10a] That is, we have restricted our attention to the initial intermediate-to-maximum portions of the buildup curve and numerically solved the volume matrix at each mixing time. In this approach, no assumptions are made concerning isolated spin systems or indirect spin transfer.[11]

Table VI gives the ^{1}H chemical shifts and coupling constants for CTA ($CDCl_3$, 25 and 60 °C), CTP ($CDCl_3$, 25 °C), and CTB ($CDCl_3$, 25 °C). Figure 3 shows a stack plot of a NOESY spectrum for CTA (0.35 M, $CDCl_3$, 25 °C) at a mixing time of 100 ms. In Figure 3, the diagonal elements correspond to the 1D ^{1}H NMR spectra and the off-diagonal elements (cross peaks) represent through-space interactions between protons from which distance information can be extracted. The peak volumes of both the diagonal and cross peaks vary as a function of mixing time. With increasing mixing time the peak volumes of the diagonal peaks decay while the peak volumes of the cross peaks increase until they reach a maximum after which they also decay. Figure 4 shows a column slice taken through the H4 diagonal peak from four CTA (0.35 M, $CDCl_3$, 25 °C) NOESY spectra illustrating the decay of the H4 diagonal peak and the corresponding increase in the volumes of the cross peaks dipolar coupled to H4.

Because of the close chemical shifts of H1 and $H6_S$, the potential for diagonal-peak and cross-peak overlap in the NOESY spectra of these triesters is apparent. For CTA at 0.35 M/25 °C and 0.1 M/60 °C, the volumes of both the H1 and $H6_S$ diagonal peaks could be directly determined. For CTA at 0.1 M/25 °C, CTP, and CTB, we could not resolve the H1 and $H6_S$ diagonal peaks. However, in the two cases where the H1 and $H6_S$ diagonal peak volumes could be directly determined, we observed that the $H6_S$ and $H6_R$ diagonal peak volumes were nearly the same. On the basis of this observation, we scaled the combined diagonal peak volumes for H1–$H6_S$ to the $H6_R$ diagonal peak volume for the three sets of data where H1 and $H6_S$ could not be directly determined.[12] One potential site for cross-peak overlap is between the $H6_S$–H3 and H1–H3 cross peaks. However, the corresponding distance for $H6_S$–H3 obtained from X-ray analysis for CTA[13] is a minimum of 4.30 Å (Table VII). Since one does not expect to see cross peaks in NOESY spectra for protons more than 4.0 Å apart,[14] we assumed that the volume for the $H6_S$–H3 cross peak was zero in all cases. This assumption was reinforced by the fact that a $H6_R$–H3 cross peak was never observed in any of our

(11) This approach assumes that the motion of the polymer is anisotropic, a condition that we have shown that these polymers meet, and that the dynamics of all of the protons present in the polymer are similar.

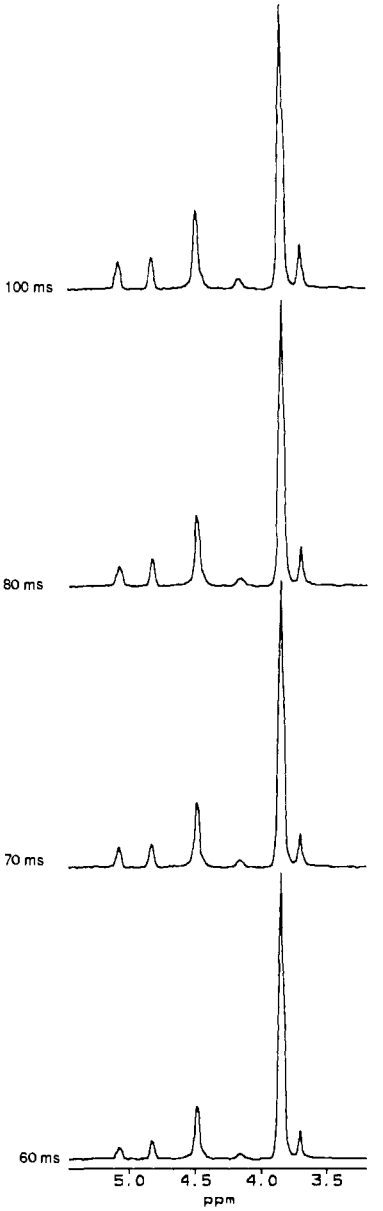

Figure 4. Column slices taken through H4 (CTA, 0.35 M, 25 °C).

Table VII. Cellulose Triacetate X-ray[a] Proton–Proton Distances (angstroms)

H1–H3	2.76	H3–H5	2.53	H2–H4	3.13	H1–H5	2.15
H3–H4	3.16	H4–H5	2.95	H2–H5	3.89	H1–H2	3.00
H3–H2	2.99	H1–H4	3.98	H6A–H1	5.03	H6B–H1	3.85
H6A–H2	6.39	H6B–H2	5.29	H6A–H3	4.30	H6B–H3	4.72
H6A–H4	2.79	H6B–H4	3.58	H6A–H5	2.45	H6B–H5	2.29
H6A–H6B	1.70						

[a] Taken from ref 13.

(12) Macura, S.; Farmer, B. T.; Brown, L. R.; Ernst, R. R. *J. Magn. Reson.* **1986**, *70*, 493–499.
(13) Stipanovic, A. J.; Sarko, A. *Polymer* **1978**, *19*, 3–8.
(14) Ernst, R. R.; Bodenhausen, G.; Wokum, A. *Principles of Nuclear Magnetic Resonance in One and Two Dimensions*; Oxford Scientific Publications: Oxford, 1986.

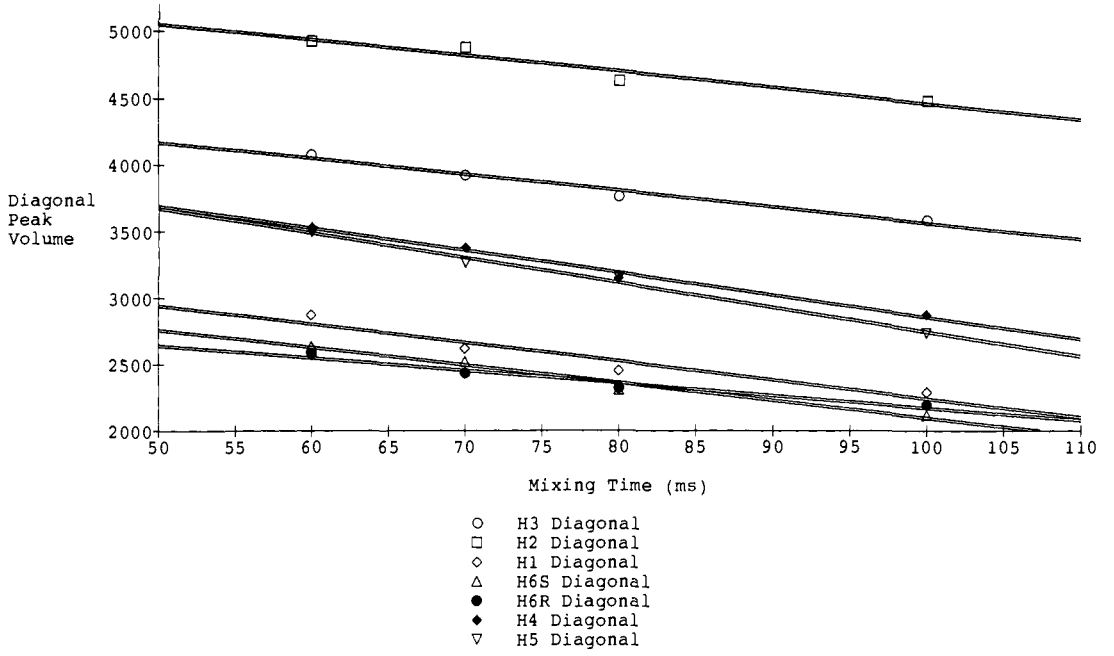

Figure 5. CTA diagonal peak decay (0.35 M, 25 °C).

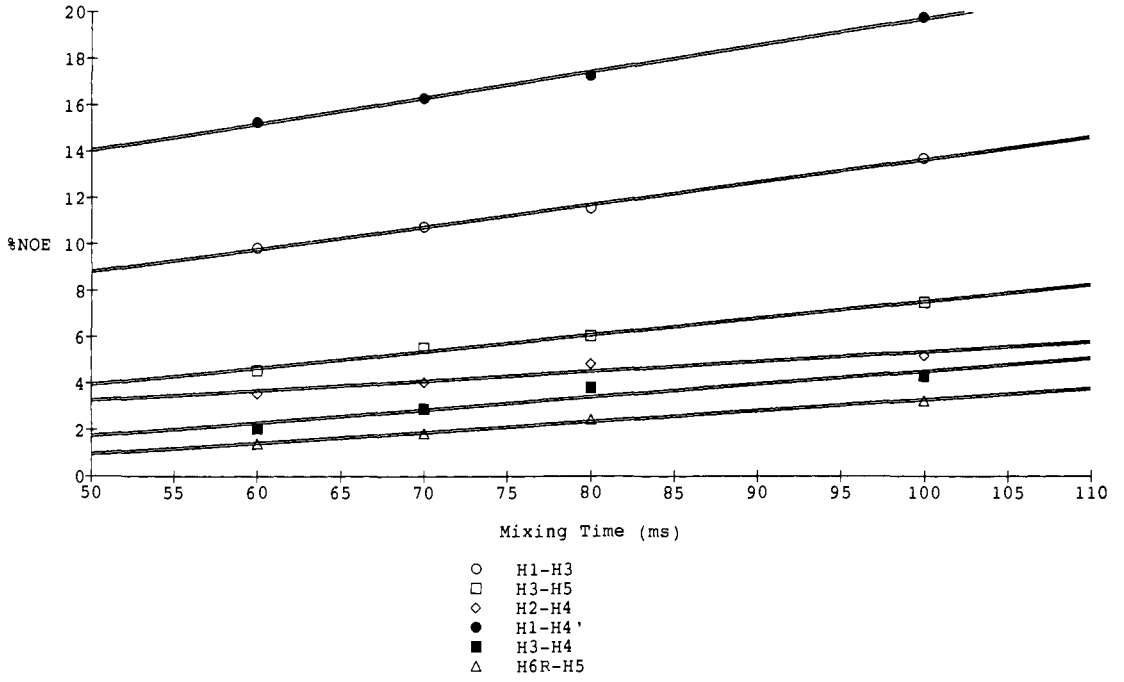

Figure 6. CTA NOE cross-peak buildup (0.35 M, 25 °C).

NOESY spectra. Similarly, the $H6_R$–H1 cross peak would lie underneath the $H6_R$–$H6_S$ cross peak, the $H6_S$–H1 cross peak would be too close to the diagonal to be observed, and the $H6_S$–H2 cross peak would overlap with H1–H2 ($H6_R$–H2 is not observed). X-ray analysis (Table VII) also suggests that these distances are too large for a cross peak to be observed in a NOESY spectrum, and hence we have assumed these peak volumes to be zero. There is also the potential for $H6_S$–H5,4′ cross-peak overlap with the H1–H5,4′ cross peaks. Indeed, Table VII shows that we should expect to observe these interactions. Moreover, the $H6_R$–H5,4′ cross peaks are observed for CTA, CTP, and CTB. In these instances, our only recourse was to assume that the $H6_R$–H5,4′ and $H6_S$–H5,4′ cross peaks will be equal in volume and to use the $H6_R$–H5,4′ cross peaks to scale the H1–H5,4′ cross peak volumes accordingly. Finally, there is also the potential for an intramolecular contribution (H1–H4) to the H1–H4′ cross peak. Table VII shows that the H1–H4 distance is too large for this interaction to make a significant contribution to the H1–H4′ cross peak volume.

In this work, we have acquired three sets (0.35 M/25 °C, 0.1 M/25 °C, and 0.1 M/60 °C) of NOESY spectra for CTA at four mixing times. In addition, sets of NOESY spectra for CTP (0.09 M/25 °C) and CTB (0.08/25 °C) at four mixing times were acquired. Figure 5 shows the decay of the diagonal peaks for CTA at a concentration of 0.35 M at 25 °C while Figure 6 shows the NOE buildup for selected cross peaks from this data set (for clarity we have not attempted to present all of the cross peaks.).

The set of NOESY spectra for CTA at 0.1 M/60 °C contains some unique features. Relative to CTA at 0.1 M/25 °C, the NOE buildup occurred at longer mixing times (90–200 ms at 60 °C vs 40–100 ms at 25 °C) and the peak volumes were smaller. Moreover, due to a temperature-induced change in effective correlation times, only the cross peaks between protons with a 1,3-syn relationship (e.g., H1–H3) were of the same phase as the

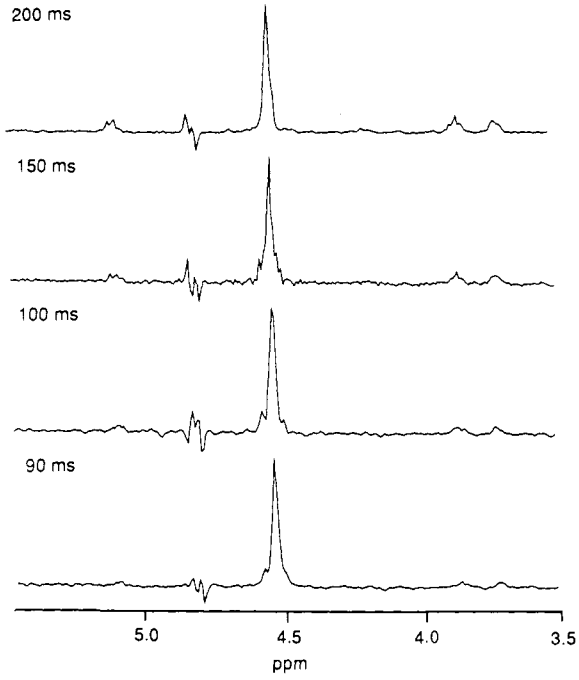

Figure 7. Column slices taken through H1 (CTA, 0.1 M, 60 °C).

diagonal peaks. Cross peaks between protons with longer range interactions either vanished or became oppositely phased to the diagonal (Figure 7). Since a comparison between CTA at 25 °C and CTA at 60 °C is valid only for protons with similar dynamics, we retained only the peak volumes for the cross peaks that were of the same phase as the diagonal peaks in calculating the rate matrices for the 60 °C data set.

The peak volumes at zero mixing time were obtained by extrapolating the diagonal peak volumes to zero mixing time. Calculation of the rate matrices at each mixing time provided cross-relaxation rates that were used to calculate interproton distances. In calculating interproton distances, we utilized the geminal protons at C6 as our pair of fixed protons and assumed a separation distance of 1.70 Å (Table VII). In each data set, the average rates for each interaction were used to calculate an interproton distance. The distances at each mixing time were then used to calculate an average distance and distance range (Table VIII).

The most striking feature of the data in Table VIII is the basic similarity of the proton–proton distances for each entry. For the ring protons, there are slight differences. However, given the small energy differences between slightly differing chair conformations (of which we "see" only the average) and the consistency of the ^1H coupling constants, we must conclude that these substituents, temperatures, and concentrations do not perturb the basic $^4C_1$ chair conformation.

Table VIII does not provide sufficient data for determination of the familiar torsion angles about the glycosidic bond. We can, however, estimate the virtual angle, θ, between H1 and H4′ of each cellobiose subunit (Figure 8), which represents the deviation of H4′ from a syn planar relationship with H1. X-ray studies of CTA fiber have shown that both CTA I and CTA II can be represented as 2/1 helices.[13,15] Using models, we restricted the anhydroglucose ring to a rigid $^4C_1$ conformation and constrained the atoms H1–C1–O_g–C4′–H4′ to a syn planar conformation (a 2/1 helix), which allowed us to measure an internuclear distance of 1.8 Å between H1 and H4′. If we rotate ring B about the O_g–C4′ bond while holding ring A fixed, we can use the data from Table VIII to estimate θ. By this method, we have estimated the virtual angle for these cellulose esters to be 30–34°. This suggests that approximately 2.5 cellobiose units (5 glucose monomers) are required for H1 to rotate through 360° (a 5/4 helix). This observation is consistent with the work of Ritcey and Gray, who used induced circular dichroism to probe the helical conformation of cellulosic chains.[16]

Table VIII. Cellulose Triesters Solution Proton–Proton Distances and Distance Ranges (angstroms)

	CTB[a] 25 °C/ 0.08 M	CTP[b] 25 °C/ 0.09 M	CTA[b] 25 °C/ 0.1 M	CTA[b] 60 °C/ 0.1 M	CTA[b] 25 °C/ 0.35 M
H1–H4′	2.15	2.11	2.17	2.16	2.08
	2.14–2.16	2.09–2.13	2.15–2.19	2.14–2.18	2.06–2.10
H1–H3	2.22	2.25	2.39	2.28	2.24
	2.21–2.23	2.21–2.29	2.36–2.42	2.27–2.29	2.22–2.26
H3–H5	2.58	2.73	2.76	2.85	2.57
	2.54–2.62	2.65–2.81	2.70–2.82	2.82–2.88	2.52–2.63
H2–H4	2.63	2.79	2.88	3.05	2.63
	2.59–2.67	2.65–2.93	2.80–2.96	2.84–3.26	2.60–2.66
H1–H5	2.11	2.12	2.26	2.17	2.09
	2.10–2.12	2.10–2.14	2.24–2.28	2.14–2.20	2.07–2.11
H3–H4	3.13	3.35	3.46	[c]	3.01
	2.98–3.28	3.12–3.58	3.21–3.71		2.87–3.15
H4–H5	2.22	2.80	2.68	[c]	2.66
	2.19–2.25	2.69–2.91	2.64–2.72		2.62–2.70
H1–H2	3.34	3.70	3.83	[c]	3.48
	3.06–3.62	3.34–4.06	3.62–4.04		3.24–3.72
H3–H2	3.07	3.51	3.47	[c]	3.27
	3.05–3.09	3.29–3.73	3.34–3.60		3.19–3.45
H2–H5	[c]	3.89	[c]	[c]	3.62
		[d]			3.41–3.83
H6R–H5	2.69	3.07	3.14	[c]	3.04
	2.66–2.72	2.87–3.27	3.13–3.15		2.91–3.17
H6S–H5	2.69	3.08	3.15	[c]	3.17
	2.66–2.72	2.89–3.27	3.14–3.16		2.97–3.37
H6R–H4	3.08	3.50	3.84	[c]	3.45
	3.02–3.14	[d]	[d]		3.26–3.64
H6S–H4	3.08	3.52	3.87	[c]	3.40
	3.02–3.14	[d]	[d]		3.20–3.60

[a] The peak volumes that lead to these distances were determined by the method of ref 5. [b] The peak volumes that lead to these distances were determined by the method of ref 4. [c] This cross-peak interaction was not observed. [d] Only one data point was obtained.

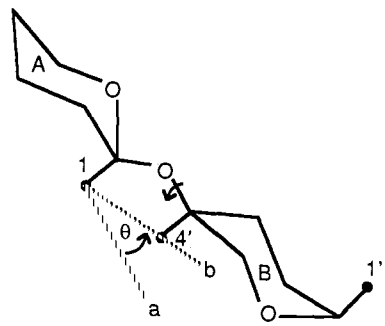

Figure 8. Cellobiose subunit where the virtual angle, θ, between H1 and H4′ represents the deviation of H4′ from a syn planar relationship with H1.

Discussion

In our earlier work with the triesters of cellulose,[2a] we presented data that defined the preferred conformation of the anhydroglucose repeat units as $^4C_1$ and proposed that these cellulose triesters exhibited left-handed helical symmetry. In addition, we noted that the choice of acyl group, solvent, or temperature had little or no effect on the proton vicinal couplings, whereas the chemical shifts were in many cases significantly affected by such changes. The changes in chemical shifts were discussed in terms of the

(15) Steinmeier, H.; Zugenmaier, P. *Carbohydr. Res.* **1987**, *164*, 97–105.

(16) Ritcey, A. M.; Gray, D. G. *Biopolymers* **1988**, *27*, 479–491. Also see: Stipanovic, A. J.; Stevens, E. S. *J. Appl. Polym. Sci., Appl. Polym. Symp.* **1983**, *37*, 277.

stereoelectronic effect of the exo oxygen (exo-anomeric effect) although changes in supramolecular structure could not be eliminated.

As we noted earlier (vide supra), the results from the present study are consistent with a $^4C_1$ conformation for the monomer units. Apparently, the choice of acyl group, concentration, or temperature does little to perturb the basic $^4C_1$ ring conformation. Furthermore, the results from this study suggest that when the acyl group or temperature is varied, change in supramolecular structure rather than in microscopic conformation is primarily responsible for the observed changes in ^1H chemical shifts. For example, at 25 °C the chemical shift order for H1 (moving upfield) is CTA, CTP, and CTB. From the NOESY data (Table VIII) we can see that the H1–H4′ distances do not follow this order as the acyl group is changed. Likewise, we also see that increasing the temperature from 25 to 60 °C shifts H1 upfield by 20 Hz while the H1–H4′ distance remains unchanged. Moreover, as we noted previously, the T_1 values of CTA change abruptly at ca. 53 °C. From Table VIII we can see that neither the basic chair conformation nor the H1–H4′ distance is affected when the interproton distances are measured below and above this transition temperature.

It seems evident that the observed changes in ^1H chemical shifts and the temperature transition in T_1 values are due to changes in supramolecular structure. However, the observed changes due to concentration are more complex. Decreasing the concentration apparently induces an interrelated change in both macroscopic and microscopic conformation. A priori, one expects an increase in T_1 values with decreasing concentration. With CTA (Table IV), a decrease in T_1 values is observed, which we interpret as an increase in chain interaction. Furthermore, the virtual angle between monomer units increases (Table VIII), which suggests that as chain interactions increase, chain helicity increases. Because of this interaction of supramolecular structure and microscopic conformation, the ^1H chemical shifts do not change significantly.

Conclusion

The concept that temperature and concentration can influence solution conformations of macromolecules is well precedented.[17] However, very few studies have been reported that have explored the effect of these variables on high polymers on both a macromolecular and microscopic level. We have shown that carbon-13 NMR relaxation time studies and 2D NOESY studies are suitable tools for probing molecular dynamics and for determining interproton distances in these polymers. Using these tools, we have shown the following: (i) The basic $^4C_1$ conformation of the anhydroglucose monomers is not significantly perturbed by acyl type, temperature, or concentration. (ii) The virtual angle between H1 and H4′ of adjacent anhydroglucose units for cellulose esters is 30–34°, which suggests that these biopolymer derivatives exist as 5/4 helices. (iii) CTA undergoes a unique transition at 53 °C that appears to be due to changes in supramolecular structure. (iv) Decreasing concentration induces a complex, interrelated change in both macroscopic and microscopic conformation.

We recognize that the data we have presented are average values for a set of low-energy conformations interconverting rapidly on the NMR time scale. Nevertheless, our work provides a set of NMR constraints that can give us guidance in constructing a concept of the actions of these polymers in solution. The next step will be to use molecular dynamics simulations to probe for discrete solution structures that will satisfy the experimental constraints.

Acknowledgment. We thank Dr. P. S. Wehner, ECD Research Laboratories, for his aid in implementing the approach of Denk, Baumann, and Wagner for the determination of NOESY peak volumes.

Registry No. 1, 9012-09-3; **2**, 39320-19-9; **3**, 39320-16-6.

(17) (a) Doty, P.; Yang, J. T. *J. Am. Chem. Soc.* **1956**, *78*, 497–500. (b) Bovey, F. A. *J. Polym. Sci., Macromol. Rev.* **1975**, *9*, 1–81. (c) Vogl, O.; Jaycox, G. D. *Polymer* **1987**, *28*, 2179–2182.

Effect of pH and Salt Concentration on Bimodal Inclusion of a Nitroxide by Cyclodextrins

Yashige Kotake* and Edward G. Janzen*

Contribution from the Department of Chemistry and Biochemistry, University of Guelph, Guelph, Ontario, Canada N1G2W1. *Received January 25, 1989*

Abstract: The effect of pH and ionic salts on the binding of bimodal inclusion complexes between cyclodextrin and a nitroxide radical probe has been examined by using ESR spectroscopy. A sharp decrease in the amount of inclusion complex relative to the free probe was observed at pH $\sim$ 12, which corresponds to the dissociative pH of protons in the hydroxyl groups on the rim of the cyclodextrin, indicating that the ionized cyclodextrin does not have the ability to include the nitroxide probe selected. The pK_a's of the hydroxyl groups of cyclodextrins are calculated to be 11.3 ± 0.8, 11.7 ± 0.4, and 11.9 ± 0.4 for α-, β-, and γ-cyclodextrin, respectively, on the basis of the pH dependence of the spectra. When an ionic salt was added to the solution of the complex of α-, β-, and γ-cyclodextrin, the association constant of the inclusion complex increases as a function of the salt concentration. The nature of the salt effect in the cyclodextrin system is discussed on the basis of the change of the enthalpy and entropy of association by the addition of salt. In addition, as the concentration of the salt is increased the inclusion of the *tert*-butyl group is enhanced more than that of the phenyl group. This result is discussed on the basis of the difference in the hydrophobicity of the included group.

The characteristics of the molecular cavity of cyclodextrin, a cyclic oligomer of glucose, have been well characterized both in the solid and solution phases.[1] In the study of host–guest complexes the effect of pH and salt on the inclusion behavior cannot be studied in the solid phase. From the viewpoint of enzyme-function-directed chemistry the study of the effect of pH and salt is especially important in understanding the phenomena such as the pH dependence of the activity, salting in, salting out, and denaturation.

Recently, Schneider et al.[2,3] studied the effect of solvent and salt on the association constants (binding constants) of organic

(1) For example, see: (a) Bender, M. L.; Komiyama, M. *Cyclodextrin Chemistry*; Springer: New York, 1978. (b) Saenger, W. *Angew. Chem., Int. Ed. Engl.* **1980**, *19*, 344. (c) *Inclusion Compounds*; Atwood, J. L., Davies, J. E. D., MacNicol, D. D., Eds.; Academic Press: London, 1984; Vols. 2 and 3.

(2) Schneider, H.-J.; Kramer, R.; Simova, R.; Schneider, U. *J. Am. Chem. Soc.* **1988**, *110*, 6442.

(3) Schneider, H.-J.; Guttes, D.; Schneider, U. *J. Am. Chem. Soc.* **1988**, *110*, 6449.

0002-7863/89/1511-7319$01.50/0